Analysis of the Effect of Trochoidal Milling on the Surface Roughness of Aluminium Alloys after Milling

Jerzy Józwik
Mechanical Engineering Faculty, Lublin University of Technology, Nadbystrzycka 36, 20-618 Lublin, Poland.
E-mail: j.jozwik@pollub.pl

The paper presents the results of the surface morphology of aluminium alloys after milling. The 3D surface roughness parameters Ra, Rz, RSm were examined. Functional relationships between the cutting forces, the torque and the roughness parameters were established. The investigation was carried out with respect to functional characteristics of the surface of aluminium alloys. Two different aluminium alloys: 2024 and 6082, were investigated. Two different milling strategies were employed: milling with a trochoidal tool path and milling with a conventional tool path. Different radial depths of cut were applied in the tests. The percentage of the radial depth of cut was increased every 5 %, from 5 % to 40 %. The results were compared with the conventional machining.

Keywords: Cutting, Surface Morphology, Roughness Parameters, Trochoidal Milling

1 Introduction

Aluminum machining is one of the more interesting shaping techniques that scientists from around the world analyse [1-15]. The tool wear, forces as well as the stability of the cutting process are mainly analyzed [1-4]. In other works [11-17] we can find noise analysis [6-8], dust concentrations during aluminium aloys machining [9], as well as the shape and form of chips [10]. In many works, electromagnetic fields [11,12] and energy characteristics of this process are analyzed [13-17]. The authors of the work [18-21] compare the trochoidal milling method with plunge milling. Selection of a milling strategy is a very important aspect of machining program design for specified parts [22-25]. It depends on factors such as the type and material of the cutter (including the coat), the length of the chuck and working part, the machine's rigidity and its kinematic capabilities, etc, [23-24]. Modern machine tools enable complete machining, i.e. machining parts with the use of only one machine, frequently provided with one or a few fixtures [22]. This is possible, among others, thanks to the use of multi-axis and multi-spindle rigid CNC machine tools. This, in turn, enables reducing the number of chucks and offers the possibility of using many complicated and efficient machining strategies, which results in a significant reduction of manufacturing time [26-29]. In addition to time savings, the accuracy of machined parts is increased too [25]. CAM software manufacturers are developing more and more efficient machining strategies, introducing new functions to facilitate processing. Gaining insight into these strategies makes it possible to optimize the cutting process and improve its efficiency [25-29].

2 Methods and test stands

The objective of this study was to determine the effect of applied milling strategies (conventional and trochoidal) on the workpiece geometry. Conventional and trochoidal tool paths were compared. Tests were performed on two different aluminium alloys: 2024 and 6082. Cutting forces and torques as well as machining times obtained for two analysed milling strategies and different cutting parameters were also compared. The radial depth of cut, ae, was variable in the milling process. The percentage of the radial depth of cut in successive test runs was increased by 5%, from 5% to 40%. The milling process was performed with the use of a coolant. Fig. 1 shows the employed milling strategies. Specimens for the tests were rectangular solids of the dimensions 60x60x50mm, made of two types of aluminium alloys. Eight specimens were prepared for the tests. Four corners with a radius of 24 mm were subjected to milling (Fig. 1). The tests were performed using a TiAlN-coated four-tooth solid carbide end mill of 12 mm in diameter, manufactured by GUEHRING.

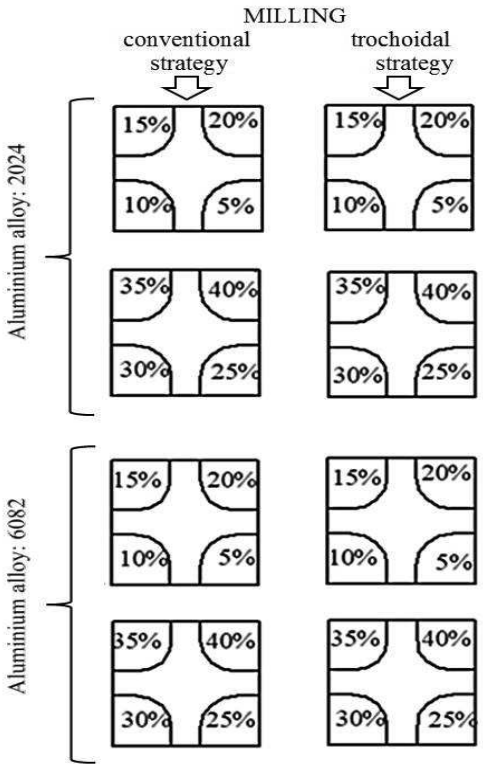

***Fig. 1** Schematic illustrating the employed milling strategies (conventional and trochoidal) in the analysis of specimens of the analysed aluminium alloys: 2024 and 6082*

The following technological parameters were applied in the analysed milling strategies: the cutting speed, v_c = 650 m/min (the spindle speed, n = 17000 rev/min), the feed per tooth, f_z = 0.03 mm/tooth (the feed rate, v_f = 2070 mm/min). In trochoidal machining, the axial depth of cut, a_p, was set equal to 25mm, while in conventional machining it was set at 6.25mm. The process was performed with the use of a cooling lubricant. Based on the results of profile roughness after machining, selected surface roughness parameters of the specimens were compared. The portable HOMMEL TESTER T1000 was used to measure profile roughness after machining. Surface roughness measurements were performed with the cutting speed v_t of 0.5mm/s; the measuring range was set at 80μm, the sampling length, *Lc*, was set at 0.8mm, while the total measuring length was set equal to 4.8mm. A trochoid is the curve traced out by a point fixed to a circle as it rolls along a straight line. The point may be inside or outside the circle. 6 different types of trochoids can be distinguished. Depending on their shape, they can be classified as inside and outside curves [12]. Inside trochoids include hypocycloid and hypotrochoid curves. The latter can be contracted or extended. Epicycloids as well as contracted and extended epitrochoids can be classified as inside trochoid curves. A hypocycloid is a special case of a hypotrochoid, and is described by the quotient R/r equal to 3 (this curve is also known as a deltoid) [12].

Fig. 2 shows the conventional and trochoidal tool paths, designed in CAM. The two tested milling strategies were simulated, and their cutting times were determined (Fig. 3).

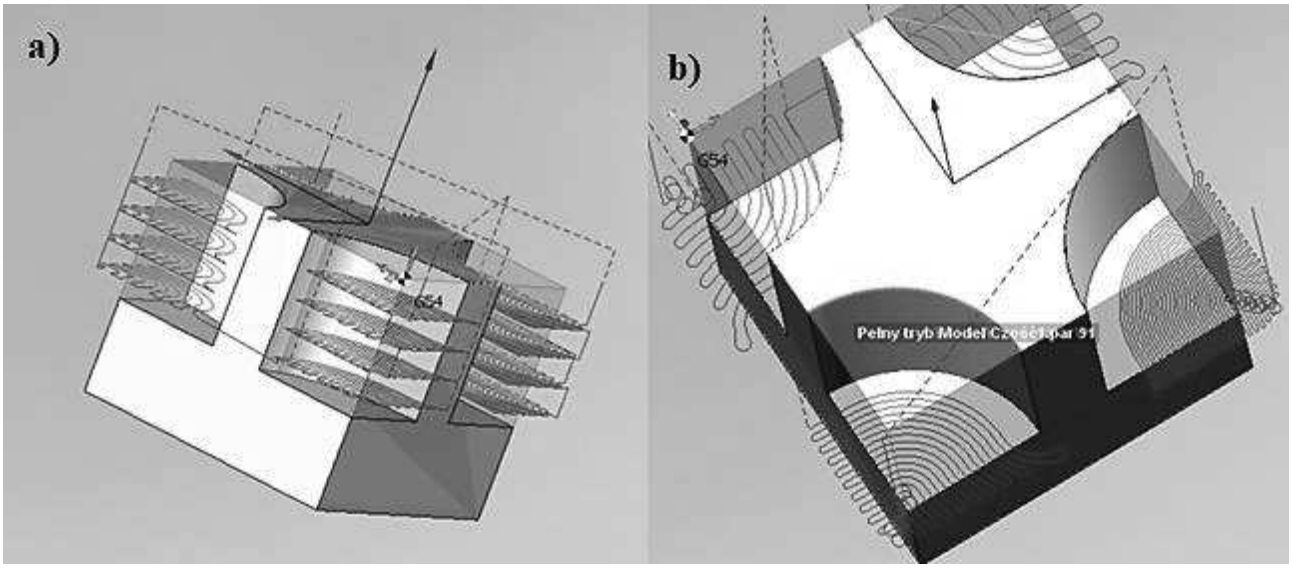

Fig. 2 *Tool paths: a) conventional milling strategy, b) trochoidal milling strategy*

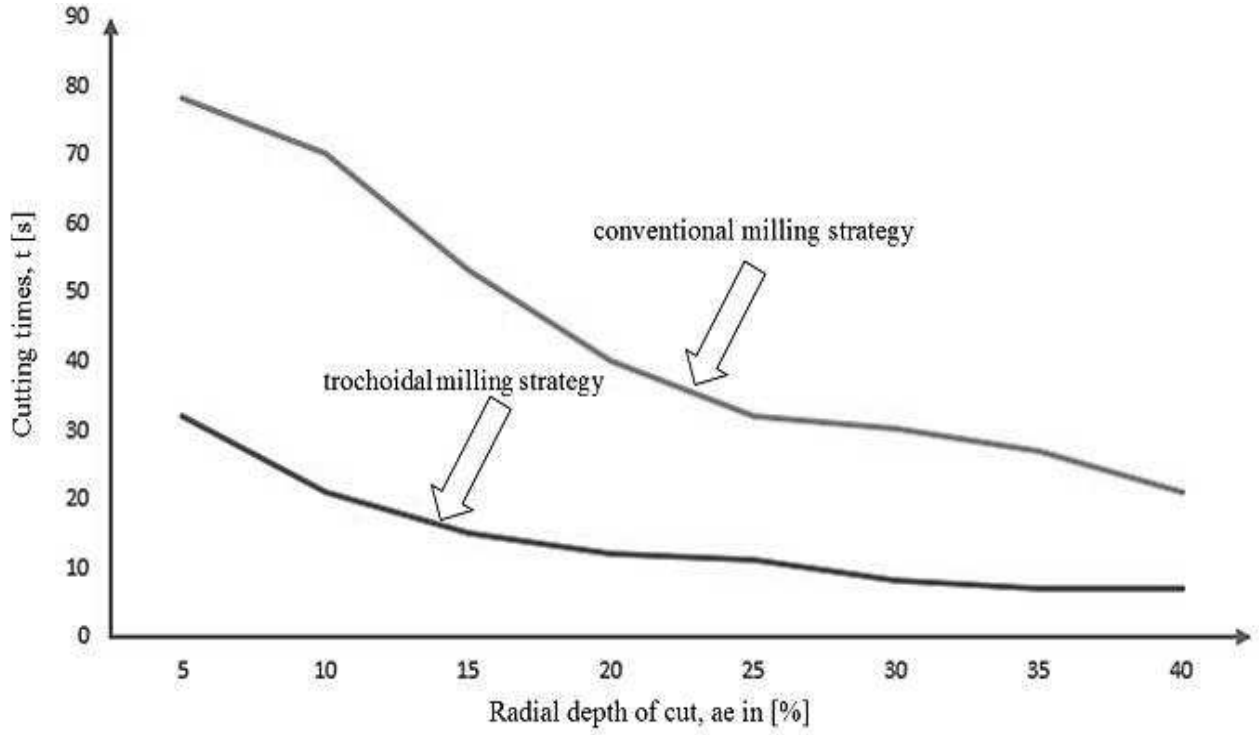

Fig. 3 *Cutting times in conventional and trochoidal milling strategy*

Each of the 6 curves is determined based on Eqs. (1) and (2), which for inside trochoids are written as:

$$\boldsymbol{x = (R - r)\cos(t) + h\cos\left(\frac{R-r}{r}t\right)} \quad (1)$$

$$x = (R - r)\sin(t) - h\sin\left(\frac{R-r}{r}t\right) \quad (2)$$

Where:
R - is the radius of the outside circle,
r - is the radius of the inside (rotating) circle,
h - is the distance between the point and the centre of the inside circle (in this case, it is equal to r).

In the case when h=r, the curve has the form of a hypocycloid. If h>r an extended hypotrochoid is created, and if h<r – a contracted hypotrochoid is obtained. A general formula for outside trochoids is given by Eqs. (3) and (4):

$$\boldsymbol{x = (R + r)\cos(t) + h\cos\left(\frac{R+r}{r}t\right)} \quad (3)$$

$$x = (R + r)\sin(t) - h\sin\left(\frac{R+r}{r}t\right) \quad (4)$$

Where:
R - is the radius of the outside circle,
R - is the radius of the inside (rotating) circle,
h - is the distance between the point and the centre of the inside circle (in the below case it is equal to r).

An epicycloid is a special case of an epitrochoid. Below is shown an epicycloid curve with the quotient R/r equal to 2 (this curve is also known as a nephroid) [12]. In the case when h = r, the curve has the form of an epicycloid; if h > r an extended epitrochoid is obtained, and if h < r – a contracted epitrochoid is generated. Trochoidal curves are very useful not only for generating tool paths in CAM, but they are also used in other industrial branches, for instance in the manufacturing of engines in which the piston moves along an epitrochoid curve, e.g. the Wankel engine [12].

Following the selection of milling strategies and tool paths, a CNC code was generated using a postprocessor. Once the workpiece and the tool had been fixed, the milling process was started. The milling was performed on the AVIA VMC800HS machining centre. Cutting forces and torques were measured with the KISTLER 9123 dynamometer.

3 Results analysis and discussion

3.1 Analysis of the specimen geometry

The experimental tests provided results of the profile roughness parameters Ra, Rz and RSm. Surface roughness was measured in three sampling points (1, 2, 3), on the surface of every machined corner: at the entrance of the tool into the material, in the centre of the material, and at the exit of the tool from the material (Fig. 4).

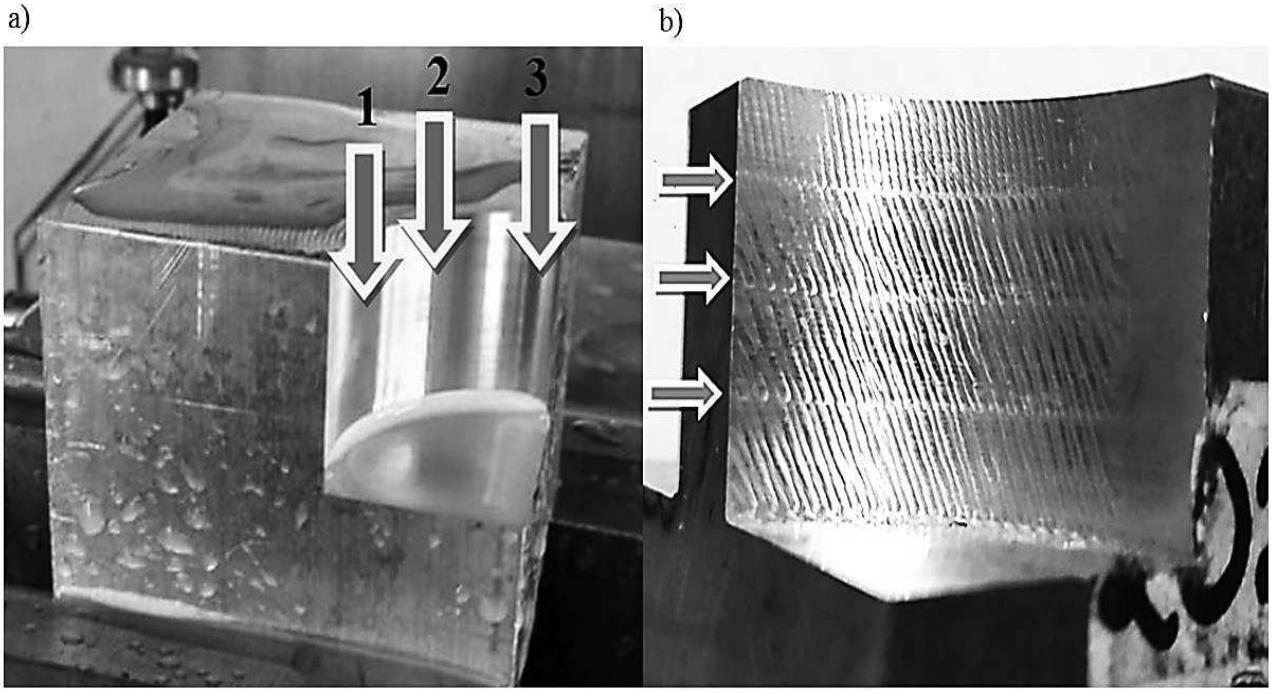

Fig. 4 *Profile roughness sampling points*

After that, the results were averaged and compared with successive results. Tab. 1 lists the mean values of the analysed surface parameters, and Tab. 2 lists the mean results of the material sampled in 8 corners, for the two analysed milling strategies.

The same set of roughness parameters were examined in every test. An analysis of obtained results demonstrates that all tested surface roughness parameters increase with increasing the radial depth of cut *ae* during the milling process. This increase occurs in both tested milling strategies (conventional and trochoidal), for aluminium alloy 2024 and aluminium alloy 6082 alike. The only exception is the mean width of the profile elements, RSm.

Tab. 1 *Surface roughness parameters, depending on the aluminium alloy type and employed milling strategy*

Aluminium alloy 2024				Aluminium alloy 6082			
Trochoidal milling strategy				Trochoidal milling strategy			
ae [%]	Ra [μm]	Rz [μm]	RSm [mm]	*ae* [%]	Ra [μm]	Rz [μm]	RSm [mm]
5	0.752	4.443	0.089	5	0.711	4.377	0.116
10	0.767	4.343	0.113	10	0.782	4.93	0.074
15	1.011	6.013	0.146	15	0.798	4.677	0.103
20	0.913	5.013	0.127	20	0.83	5.12	0.093
25	1.185	6.473	0.212	25	1.166	6.17	0.161
30	1.125	5.42	0.215	30	1.155	6.42	0.147
35	1.489	7.163	0.248	35	1.535	7.827	0.196
40	1.875	8.487	0.361	40	2.141	10.603	0.273
Conventional milling strategy				Conventional milling strategy			
ae [%]	Ra [μm]	Rz [μm]	RSm [mm]	*ae* [%]	Ra [μm]	Rz [μm]	RSm [mm]
5	0.794	4.897	0.109	5	0.881	5.24	0.101
10	0.874	5.133	0.1	10	0.963	5.727	0.119
15	1.036	6.557	0.115	15	0.888	5.337	0.098
20	1.068	5.993	0.169	20	0.984	6.45	0.121
25	0.954	5.447	0.132	25	1.381	6.96	0.188
30	1.172	6.437	0.203	30	1.433	7.957	0.186
35	1.772	8.51	0.362	35	1.45	6.9	0.231
40	1.294	7.14	0.186	40	1.432	7.997	0.176

Tab. 2 *Mean roughness parameters, depending on the milling strategy and material type (aluminium alloy 2024, aluminium alloy 6082)*

Trochoidal milling strategy; Aluminium alloy 2024			Trochoidal milling strategy; Aluminium alloy 6082		
Ra [μm]	Rz [μm]	RSm [mm]	Ra [μm]	Rz [μm]	RSm [mm]
1.140	5.919	0.189	1.140	6.266	0.145
Conventional milling strategy; Aluminium alloy 2024			Conventional milling strategy; Aluminium alloy 6082		
Ra [um]	Rz [μm]	RSm [mm]	Ra [μm]	Rz [μm]	RSm [mm]
1.121	6.264	0.172	1.177	6.571	0.153

In trochoidal milling, the RSm parameter gradually increases with increasing the radial depth of cut *ae*; in conventional milling, however, this parameter changes in a random (stochastic) manner, reaching its maximum value at the radial depth of cut *ae* of 35%, for both tested aluminium alloys (2024 and 6082). A comparison of the mean values listed in Tab. 2 reveals that they slightly differ, depending on the employed milling strategy. However, these difference do not exceed 10%. In trochoidal milling, the Rz parameter is lower by approx. 5 – 6%. The Ra parameter is higher by 1 – 3% in conventional milling. In trochoidal milling, the Rsm parameter is higher by 9% for aluminium alloy 2024, while for aluminium alloy 6082 – it is lower by 5%. A comparison of the results of the surface roughness parameters in conventional and trochoidal milling is given in Fig. 5.

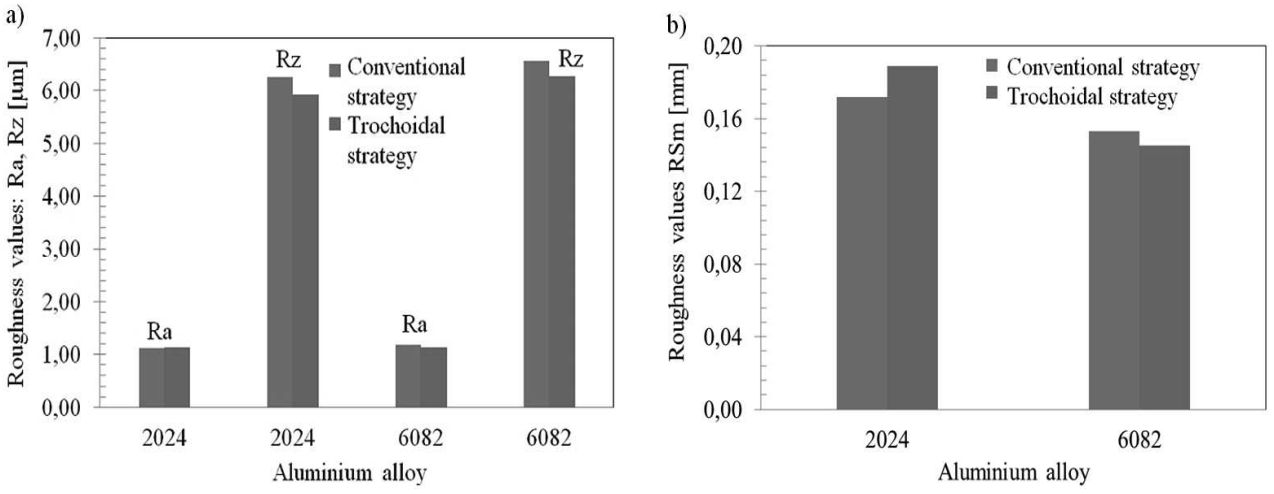

Fig. 5 *Comparison of mean values of surface roughness parameters obtained in conventional and trochoidal milling of aluminium alloys 2024 and 6082: a) Ra and Rz, b) RSm*

In conventional milling one can visibly notice tool pass traces. It can be observed that with increasing the radial depth of cut, the traces become more visible and the surface roughness significantly increases. An inspection of specimens subjected to trochoidal milling reveals the presence of slight flaking of the material probably resulting from very high values of the roughness parameter, which made it impossible to remove chips from the cutting zone.

3.2 Analysis of the cutting forces and torques

The study investigated the cutting forces and torques in the cutting of aluminium alloys 2024 and 6082. For every test, a representative time interval was selected for analysis. In the conventional milling of aluminium alloy 2024 the cutting forces range between 40 N and 120 N, and the maximum torque does not exceed 1.2 Nm. The cutting forces increase with increasing the radial depth of cut *ae* during milling. In the trochoidal milling of aluminium alloy 6082, the cutting forces also range from 40 N to 140 N. However, the highest cutting forces can be observed when the radial depth of cut (*ae*) is set at 25-30 %, while at the radial depth of cut *ae* of 35 % the cutting force does not exceed 100N. Fig. 6 shows the plots of cutting forces and torques obtained for aluminium alloy 2024 at the radial depth of cut *ae* of 40 % in conventional milling (Figs. 6a 6b) and trochoidal milling (Figs. 6c and 6d). Fig. 6 demonstrates that the reactive cutting force in conventional milling ranges from 45 N to 110 N, while the cutting torque is between 0.25 Nm and 1.2 Nm. The amplitude of forces changes with changing the torque and amounts to 60N. The higher the torque is, the higher the cutting force amplitude becomes. For the torque of 1 Nm, the amplitude of cutting forces is 60 N, while for the torque ranging 0.45-0.6 Nm, the cutting force amplitude is between 30 N and 50 N.

Fig. 7 shows the cutting forces and torques obtained for aluminium alloy 2024 at the radial depth of cut *ae* of 40 % in conventional milling (Figs.7a and 7b) and trochoidal milling (Figs.7c and 7d). The results demonstrate that the reactive cutting force and torque in trochoidal milling are on average three times higher than in conventional milling. This results from the nature of the trochoidal strategy. It must, however, be highlighted that the application of the above milling strategy increases the process efficiency by three times (Fig. 3).

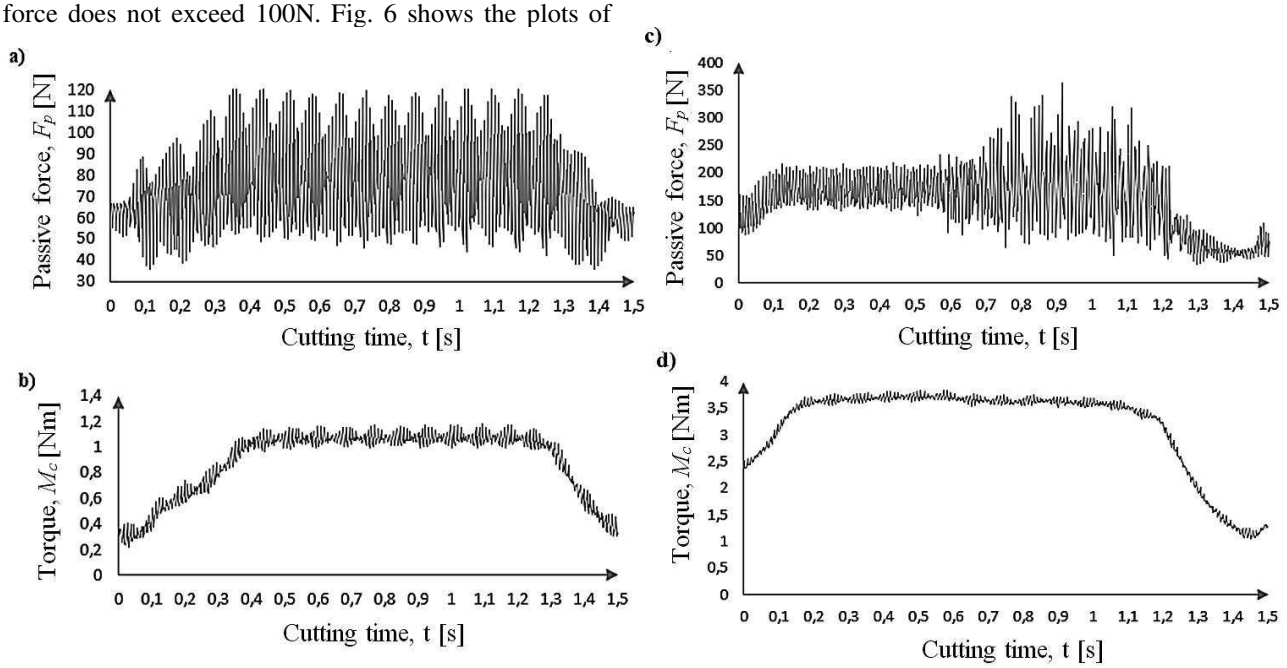

Fig. 6 *Cutting forces (passive) and torques obtained in the milling of aluminium alloy 2024: a) reactive component at the radial depth of cut ae of 40 % (conventional), b) torque at the radial depth of cut ae of 40% (conventional), c) reactive component at the radial depth of cut ae of 40 % trochoidal), d) torque at the radial depth of cut ae of 40% (trochoidal)*

In conventional milling, as the tool cuts into the material, the forces gradually increase and then reach a stabilized value. Once the tool has cut into the workpiece entirely, the forces and the amplitude of forces become stabilized. The reactive cutting force and torque slightly increase with increasing the radial depth of cut *ae*. The lower the cutting torque is, the lower the amplitude of cutting forces becomes. With increasing the cutting torque, the cutting force amplitude increases too.

Interesting results of the cutting force and torque have been obtained in trochoidal milling with the radial depth of cut (*ae)* set at 15 % and 20%. Fig. 8 shows the plots of cutting force and torque for aluminium alloy 6082. The results demonstrate that the reactive cutting force and torque in trochoidal milling are on average three times higher than in conventional milling. This results from the nature of the trochoidal strategy. It must, however, be highlighted that the application of the above milling strategy increases the process efficiency by three times (Fig. 3). In conventional milling, as the tool cuts into the material, the forces gradually increase and then reach a stabilized value.

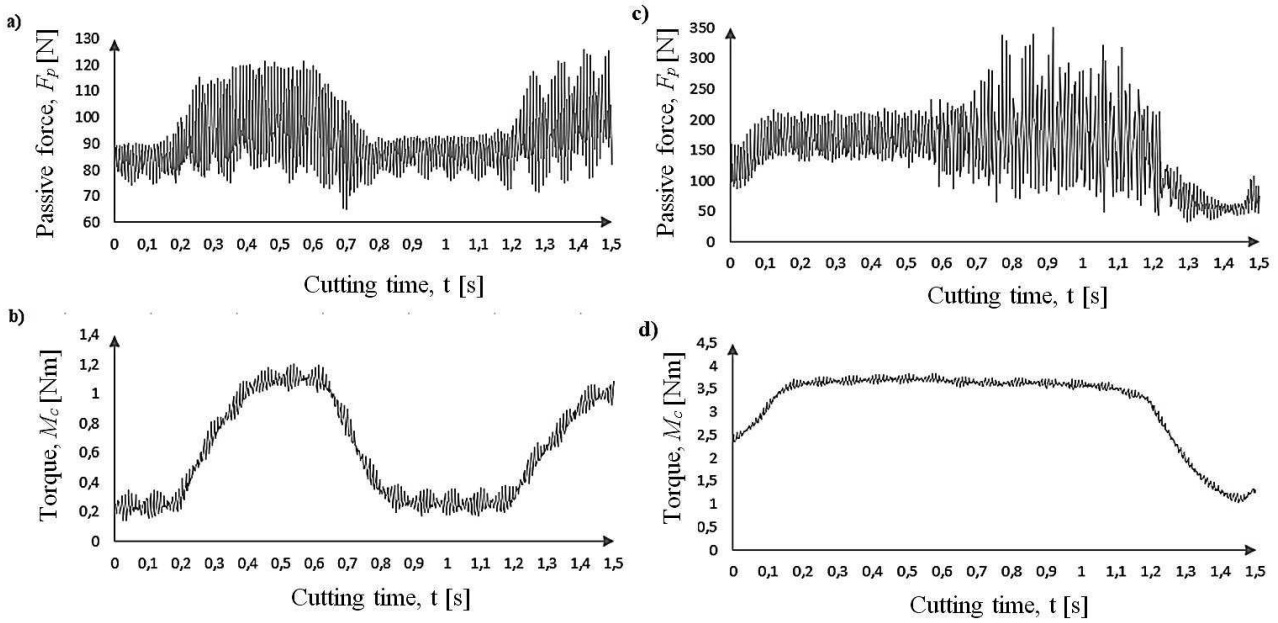

Fig. 7 *Cutting forces (passive) and torques obtained in the milling of aluminium alloy 6082: a) reactive component at the radial depth of cut ae of 40 % (conventional), b) torque at the radial depth of cut ae of 40% (conventional), c) reactive component at the radial depth of cut ae of 40 % (trochoidal), d), torque at the radial depth of cut ae of 40% (trochoidal)*

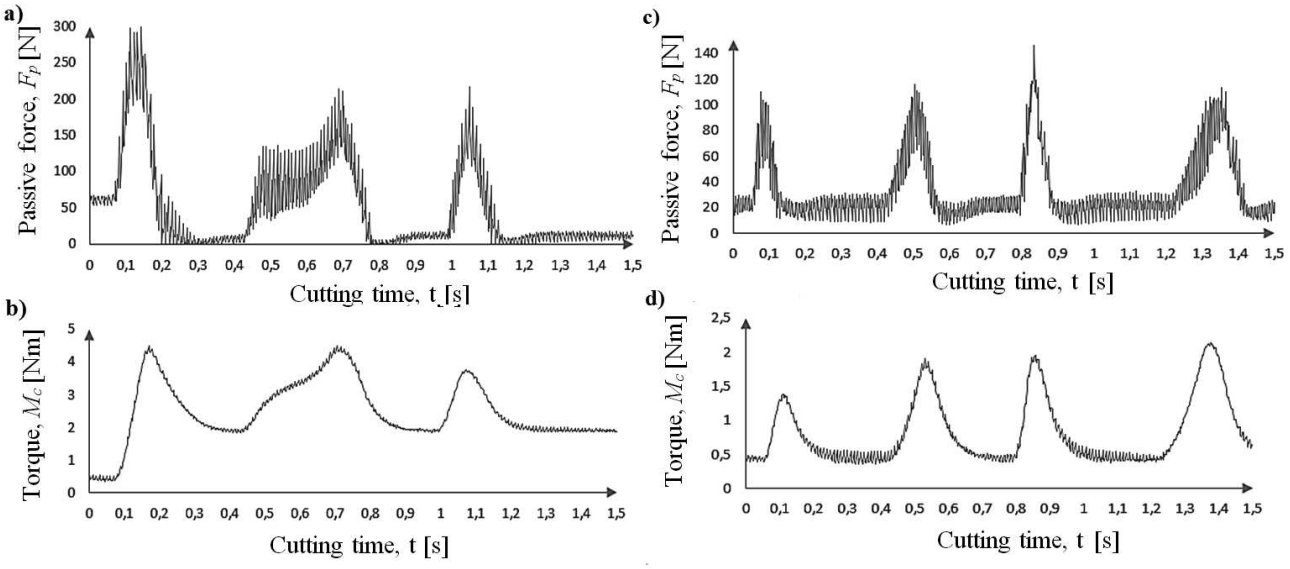

Fig. 8 *Cutting forces and torques: a) reactive component at the radial depth of cut ae of 40 % (conventional milling; aluminium alloy 2024), b) torque at the radial depth of cut ae of 40% (conventional milling; aluminium alloy 2024), c) reactive component at the radial depth of cut ae of 40 % (trochoidal milling; aluminium alloy 6082), d), torque at the radial depth of cut ae of 40% (trochoidal milling; aluminium alloy 6082).*

Once the tool has cut into the workpiece entirely, the forces and the amplitude of forces become stabilized. The reactive cutting force and torque slightly increase with increasing the radial depth of cut *ae*. The lower the cutting torque is, the lower the amplitude of cutting forces becomes. With increasing the cutting torque, the cutting force amplitude increases too. Interesting results of the cutting force and torque have been obtained in trochoidal milling with the radial depth of cut (*ae*) set at 15 % and 20%. Fig. 8 shows the plots of cutting force and torque for aluminium alloy 6082. Specifically, the plots show the reactive component at the radial depth of cut *ae* of 40% in conventional milling (Fig. 8a), the torque at the radial depth of cut *ae* of 40% in conventional milling (Fig. 8b), the reactive component at the radial depth of cut *ae* of 40 % in trochoidal milling (Fig. 8c), and the torque at the radial depth of cut *ae* of 40% in trochoidal milling (Fig. 8d).

4 Conclusion

The roughness results of the tested samples demonstrate that the Rz parameter in conventional milling is

slightly lower (5 – 6 %) than that obtained in trochoidal milling. The other parameters (Ra, Rsm) are similar. As for machining time, one can observe differences between the unit machining times. Compared to conventional machining, the trochoidal machining time is by 2.5 to 4 times shorter (approx. by 3 times, Fig. 3). The maximum forces in conventional machining range between 40 N and 140 N, with the torque amounting up to 1.5 Nm, whereas in trochoidal milling the forces range from 25 N to 300 N and the torque is close to 4 Nm. A comparison of the results reveals that both the reactive cutting force and the torque are almost three times higher. Nevertheless, it must be noted that in trochoidal machining, the radial depth of cut in one pass is four times higher than in conventional milling. Summing up the above, it can be stated that the trochoidal milling strategy is much more favourable because of its much shorter machining time and only slightly higher surface roughness. As the radial depth of cut is increased, the forces, torque and surface roughness increase too. The optimal percentage of the radial depth of cut (*ae*) in trochoidal machining (with respect to machining time, surface roughness, cutting forces and torque) ranges from 15% to 30%. At lower radial depths of cut, the milling process is significantly longer, which does not improve the roughness parameters. When the radial depth of cut (*ae*) exceeds 30%, the cutting forces increase significantly, which also affects the load and service life of the tool. The use of modern operating systems, processing technologies and machine tools ensures very accurate control and monitoring of milling processes. In effect, the cost–effectiveness of these processes is higher thanks to their enhanced optimization as well as the possibility of implementing new strategies and machining methods.

References

[1] BABAK, S., POPOV, A. (2017). The effect of the tool wear on the correlation of forces on the face and flank surfaces of the cutting tool. In: *Manufacturing Technology*, Vol. 17, No. 3, pp. 283 – 287. FME JEPU, Usti nad Labem, Czech Republic.

[2] BOLAR, G., DAS, A., JOSHI, S-N. (2018). Measurement and analysis of cutting force and product surface quality during end-milling of thin-wall components. In: *Measurement*, Vol. 121, pp. 190 – 204. Elsevier. Netherlands.

[3] HRICOVA, J., NAPRSTKOVA, N. (2015). Surface roughness optimization in milling aluminium alloy by using the Taguchi´s design of experiment. In: *Manufacturing Technology*, Vol. 15, No. 4, pp. 541 – 546. FME JEPU, Usti nad Labem, Czech Republic.

[4] HUANG, Y., YUAN, J. (2015). Milling stability prediction on small radial immersion – comparison SD Method and ZOA Method. In: *Manufacturing Technology*, Vol. 15, No. 2, pp. 136 – 143. FME JEPU, Usti nad Labem, Czech Republic.

[5] IBARAKI, S., YAMAJI, I., MATSUBARA, A. (2010). On the removal of critical cutting regions by trochoidal grooving. In: *Precision Engineering*, Vol. 34, No. 3, pp. 467 – 473. Elsevier. Netherlands.

[6] JÓZWIK, J., OSTROWSKI, D., JAROSZ, P, MIKA, D.(2016). Industrial robot repeatability testing with high speed camera phantom v2511. In: *Advances in Science and Technology - Research Journal*, Vol. 10, No.32, pp. 86–96. Lublin University of Technology. Poland.

[7] JÓZWIK, J., OSTROWSKI, D., MILCZARCZYK, R., KROLCZYK, G.-M. (2018). Analysis of relation between the 3D printer laser beam power and the surface morphology properties in Ti-6Al-4V titanium alloy parts. In: *Journal of The Brazilian Society of Mechanical Sciences and Engineering*, Vol. 40:215, pp.1 – 10, Springer. Switzerland.

[8] JÓZWIK, J., WAC-WŁODARCZYK, A., MICHAŁOWSKA, J., KŁOCZKO, M. (2018). Monitoring of the noise emitted by machine tools in industrial conditions. In: *Journal of Ecological Engineering*, Vol. 19, No. 1, pp. 83 – 93. Polish Society of Ecological Engineering. Poland.

[9] KIC, P., MÜLLER, M. (2017). Dust concentration in air during the aluminium alloy AlCu4Mg milling operations. In: *Manufacturing Technology*, Vol. 17, No. 5, pp. 729 – 733. FME JEPU, Usti nad Labem, Czech Republic.

[10] KUNDRÁK, J., GYÁNI, K., FELHŐ, C., DESZPOTH, I. (2017). The effect of the shape of chip cross section on cutting force and roughness when increasing feed in face milling. In: *Manufacturing Technology*, Vol. 17, No. 3, pp. 335 – 342. FME JEPU, Usti nad Labem, Czech Republic.

[11] MICHAŁOWSKA, J., JÓZWIK, J., MIKA, D., KRAWCZYK, A. (2017). Exposure to electromagnetic fields in the surrounding area of microtomograph for the frequency of 50Hz. In: *IEEE Eurocon 2017 -17th International Conference on Smart Technologies*, Ohrid, pp. 555-557. IEEE, USA.

[12] MIKA, D., JÓZWIK, J. (2018). Advanced time-frequency representation in voice signal analysis. In: *Advances in Science and Technology - Research Journal*, Vol. 12, No. 1, pp. 251 – 259. Lublin University of Technology. Poland.

[13] NOVÁK, M., NÁPRSTKOVÁ, N., JÓZWIK, J. (2015). Analysis of the surface profile and its material share during the grinding Inconel 718 alloy. In: *Advances in Science and Technology - Research Journal*, Vol. 9, No. 26, pp. 41–48. Lublin University of Technology. Poland.

[14] OH, N.-S., WOO, W.-S. LEE CH.-M. (2018). A study on the machining characteristics and energy

efficiency of Ti-6Al-4V in laser-assisted trochoidal milling. In: *International Journal of Precision Engineering and Manufacturing - Green Technology*, Vol. 5, No. 1, pp 37 – 45. Springer. Switzerland.

[15] OTKUR, M., LAZOGLU, I. (2007). Trochoidal milling. In: *International Journal of Machine Tools and Manufacture*, Vol. 47, No. 9, pp. 1324 – 1332. Elsevier. Netherlands.

[16] PLETA, A., MEARS, L. (2016). Cutting force investigation of trochoidal milling in nickel-based superalloy. In: *Procedia Manufacturing*, Vol. 5, pp. 1348 – 1356. Elsevier. Netherlands.

[17] PLETA, A., ULUTAN, D., MEARS, L. (2014). Investigation of trochoidal milling in nickel-based superalloy Inconel 738 and comparison with end milling. In: *ASME 2014, International Manufacturing Science and Engineering Conference collocated with the JSME 2014 International Conference on Materials and Processing MSEC2014 and the 42nd North American Manufacturing Research Conference*, Vol. 2, 9 – 13, pp. V002T02A058.

[18] RAUCH, M., DUC, E., HASCOET, J.-Y. (2009). Improving trochoidal tool paths generation and implementation using process constraints modeling. In: *International Journal of Machine Tools and Manufacture*, Vol. 49, No. 5, pp. 375 – 383. Elsevier. Netherlands.

[19] RAUCH, M., DUC, E., HASCOET, J-Y. (2009). Improving trochoidal tool paths generation and implementation using process constraints modelling. In: *International Journal of Machine Tools and Manufacture*, Vol. 49, No. 5, pp. 375 – 383. Elsevier. Netherlands.

[20] RAUCH, M., HASCOET, J-Y. (2007). Rough pocket milling with trochoidal and plunging strategies. In: *International Journal of Machining and Machinability of Materials*, Vol. 2, No. 2, pp. 161 – 175. Inderscience Publishers, Switzerland.

[21] RAUCH, M., HASCOET, J-Y. (2012). Selecting a milling strategy with regard to the machine tool capabilities: application to plunge milling. In: *The International Journal of Advanced Manufacturing Technology*, Vol. 59, No. 1– 4, pp 47 – 54. Springer. Switzerland.

[22] SALEHI, M., BLUM, M., FATH, B., AKYOL, T., HAAS, R., OVTCHAROVA, J. (2016). Epicycloidal versus trochoidal milling-comparison of cutting force, tool tip vibration, and machining cycle time. In: *Procedia CIRP*, Vol. 46, pp. 230 – 233. Elsevier. Netherlands.

[23] SHIXIONG, W., WEI, M., BIN, L., CHENGYONG, W. (2016). Trochoidal machining for the high-speed milling of pockets. In: *Journal of Materials Processing Technology*, Vol. 233, pp. 29 – 43. Elsevier. Netherlands.

[24] TOMÍČEK, J., MOLOTOVNIK, A. (2016). Influence of cutting conditions on profile milling of Inconel 738LC alloy. In: *Manufacturing Technology*, Vol. 16, No. 2, pp. 461 – 467. FME JEPU, Usti nad Labem, Czech Republic.

[25] UDDIN, M. S., MATSUBARA, A., IBARAKI, S., YASUDA, T. (2007). Comparision of cutting strategies for high productive end milling. In: *Proceedings of the 35th International MATADOR Conference - The International Machine Tool Design and Research Conference (Hinduja, S., Fan K.-Ch. (Ed.))*, pp.191 – 194. Springer. Switzerland.

[26] WASZCZUK, K.P., SKOWRONEK, H., KAROLCZAK, P., KOWALSKI, M., KOŁODZIEJ, M. (2019). Influence of the trochoidal tool path on quality surface of groove walls. In: *Advances in Science and Technology Research Journal*, Vol. 13, No. 3, pp. 38 – 42. Lublin University of Technology. Poland.

[27] WOJCIECHOWSKI, S., WIACKIEWICZ, M., KROLCZYK, G.M. (2018). Study on metrological relations between instant tool displacements and surface roughness during precise ball end milling. In: *Measurement*, Vol. 129, pp. 686 – 694. Elsevier. Netherlands.

[28] ZAGÓRSKI,I., KULISZ,M., KŁONICA, M., MATUSZAK, J. (2019). Trochoidal milling and neural networks simulation of magnesium alloys. In: *Materials*, Vol. 12, No. 13, pp. 3 – 25. MDPI. Switzerland.

[29] ZEMAN, P., BACH, P., TRMAL, G. (2017). Tool life of PM-HSS cutting tools when milling of titanium alloy In: *Manufacturing Technology*, Vol. 17, No. 1, pp. 115 – 121. FME JEPU, Usti nad Labem, Czech Republic.

10.21062/ujep/370.2019/a/1213-2489/MT/19/5/772
Copyright © 2019. Published by Manufacturing Technology. All rights reserved.